

A Family of Visible-Light Responsive Photocatalysts Obtained by Dispersing CrO₆ Octahedra into a Hydrotalcite Matrix

Yufei Zhao,^[a] Shitong Zhang,^[a] Bei Li,^[a] Hong Yan,^[a] Shan He,^[a] Lei Tian,^[a] Wenying Shi,^[a] Jing Ma,^[b] Min Wei,^{*[a]} David G. Evans,^[a] and Xue Duan^[a]

Increasing serious environmental pollution and energy shortage have become two intractable problems in the 21st century;^[1] it is, therefore, urgent to develop new materials and techniques to settle these issues.^[2] The chemistry of semiconductors has received huge attention owing to their wide application in photocatalysis, solar energy conversion, water splitting, optics, electrochemical devices and sensing.^[3–6] Titanium dioxide, the most promising photocatalyst, has been applied in areas of environment and energy.^[6,7] However, the efficient use of this kind of material is only achievable upon UV excitation in 5% solar energy, therefore, many attempts have been made to sensitize TiO₂ for the much larger visible fraction by doping with transition metal and nonmetal ions.^[8–15] These TiO₂-doped materials, in general, show limited absorption in the visible-light region, which leads to low activity.^[13,14] In addition, traditional visible-light photocatalysts are either unstable upon illumination (e.g., CdS, CdSe) or display low activity (e.g., WO₃, Fe₂O₃, In(OH)_yS_z and ZnSn(OH)₆).^[16] As a result, novel and efficient visible-light photocatalysts are highly essential to meet the requirements of future environment and energy technologies driven by solar energy.

Chromium-based inorganic materials have been widely used as catalysts for selective oxidation of various organic compounds.^[17a–d] The precipitation of chromium hydroxide is an important procedure that occurs in soil and natural water. The considerable interest in chromium hydroxides is focused on their wide technological applications in catalysis, pigment and colloid science.^[17] The structure of chromium hydroxide is based on an octahedral layer, in which one-third of the octahedral CrO₆ sites are occupied. Its structure is complementary to that of bayerite (α -Al(OH)₃) and simi-

lar to brucite-like Mg(OH)₂.^[17g] It has been reported that chromium hydroxide shows a strong absorption in the visible-light region,^[17] which implies that it could serve as potential photocatalytic material. However, no photocatalytic activity with visible-light irradiation has been found for chromium hydroxide. This is possibly related to the low efficiency of electron–hole separation or excited electron transfer. It has been reported that high dispersion of transitional metal octahedron would facilitate the electron transfer and avoid the recombination of electron and hole.^[5,7] This motivated us to take the challenge of distributing the CrO₆ octahedron unit within an inorganic matrix to enhance the efficiency of charge separation and improve photoconversion capability with visible-light irradiation.

Herein, we explored the idea of dispersing the CrO₆ octahedron unit in an inorganic hydroxide matrix using hydrotalcite. Hydrotalcites, commonly known as layered double hydroxides (LDHs), are a large class of typical layered clays, which can be described by the general formula $[M^{II}_{1-x}M^{III}_x](OH)_2(A^{n-})_{x/n} \cdot mH_2O$ (M^{II} and M^{III} are di- and trivalent cations, A^{n-} is an n -valent anion).^[18] The host structure is based on brucite-like Mg(OH)₂ layers of edge-sharing M(OH)₆ octahedra; isomorphous substitution of part of the divalent M^{II} cations by trivalent M^{III} cations generates positively charged sheets with charge-balancing anions in the interlayer gallery.^[18f–20] Recently, pioneering work by Grey et al. with the assistance of multinuclear NMR spectroscopy demonstrated that the M^{II} and M^{III} cations are distributed orderly in LDH layers.^[18a] This inspired us to disperse the CrO₆ octahedron unit with another metal octahedron at the molecular level by the formation of LDH materials; this could promote the efficiency of electron–hole separation and facilitate the transfer of excited electrons under visible light.

In this work, visible-light responsive MCr–X–LDHs ($M = \text{Cu, Ni, Zn; X} = \text{NO}_3^-, \text{CO}_3^{2-}$) were synthesized by a simple and scale-up co-precipitation method developed by our group;^[21] these were demonstrated to be effective and recyclable photocatalysts for the decomposition of organic dyes and colorless pollutants. The intrinsically electronic nature and the band gap of LDH materials were explored, which is essential for understanding the semiconductor property of Cr-containing LDHs and for their effective application in solar energy transformation. It was found that the CuCr–NO₃–LDH exhibited pronounced visible-light-response activity as well as excellent recycle ability for dye and phenols.

[a] Y. Zhao, S. Zhang, B. Li, Dr. H. Yan, S. He, L. Tian, W. Shi, Prof. M. Wei, Prof. D. G. Evans, Prof. X. Duan
State Key Laboratory of Chemical Resource Engineering
Beijing University of Chemical Technology
100029, Beijing (P. R. China)
Fax: (+86)10-64425385
E-mail: weimin@mail.buct.edu.cn

[b] Prof. J. Ma
School of Chemistry and Chemical Engineering
Key Laboratory of Mesoscopic Chemistry of MOE
Nanjing University, 210093, Nanjing (P. R. China)

Supporting information for this article is available on the WWW under <http://dx.doi.org/10.1002/chem.201101874>.

Periodic density functional theoretical calculations were carried out to study the electronic structure of these catalysts, and the results show that the band gap of the Cr-containing LDHs is attributed to the d–d transition of CrO₆ octahedron dispersed in the LDH layers with a gap of 1.6 eV; this accounts for their visible-light-response behavior. Therefore, this work not only provides a facile strategy for high dispersion of the CrO₆ octahedron within layered hydroxide matrix for the purpose of obtaining excellent visible-light activity, but also demonstrates their potential application in photocatalysis in water treatment and solar energy utilization.

MCr–X–LDHs were successfully prepared by using a method that involves separate nucleation and aging steps (SNAS) developed in our laboratory.^[21] This method consists of a very rapid mixing and nucleation process in a modified colloid mill, followed by a separate aging process, which has been successfully scaled-up in industry.^[18c] Their XRD patterns are shown in Figure 1. In each case, the reflections can

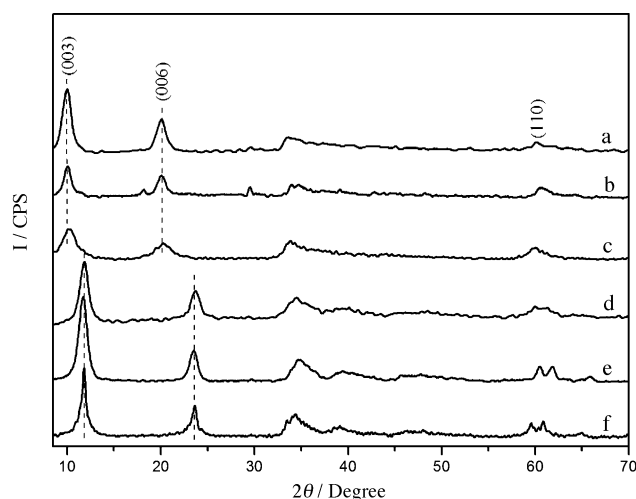


Figure 1. XRD patterns of a) CuCr–NO₃–LDH, b) NiCr–NO₃–LDH, c) ZnCr–NO₃–LDH, d) CuCr–CO₃–LDH, e) NiCr–CO₃–LDH, f) ZnCr–CO₃–LDH.

be indexed to a hexagonal lattice with *R3m* rhombohedral symmetry, commonly used for the description of LDH structures.^[22] The basal spacings of CuCr, NiCr and ZnCr–NO₃–LDH were 0.888, 0.881 and 0.867 nm, respectively, close to the value of NO₃[–]-containing LDH; the basal spacings of CuCr, NiCr, ZnCr–CO₃–LDH were 0.735, 0.791 and 0.751 nm, respectively; this is consistent with the CO₃^{2–}-type LDH. Moreover, the FT-IR spectra (Figure S1 in the Supporting Information) of these M^{II}Cr–LDHs (M = Cu, Ni, Zn) also provide evidence for the presence of NO₃[–] (at 1384 cm^{–1}) and CO₃^{2–} (at 1370 cm^{–1}), respectively. SEM images of the M^{II}Cr–LDH materials (Figure S2 in the Supporting Information) show that the particle size range is 200–500 nm. Based on these results, it can be concluded that Cr-containing LDHs were successfully prepared by using the SNAS method.

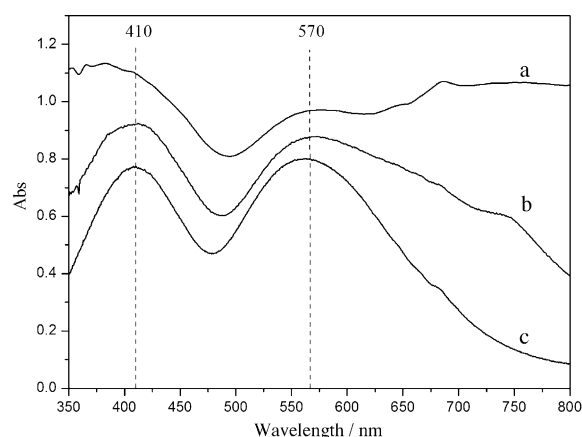


Figure 2. Diffuse reflectance UV/Vis spectra of: a) CuCr–NO₃–LDH, b) NiCr–NO₃–LDH, c) ZnCr–NO₃–LDH.

Figure 2 shows the diffuse reflectance UV/Vis spectra of the three MCr–NO₃–LDH samples. Two absorption bands in the visible region at approximately 410 and 570 nm were observed, which can be attributed to the d–d transition ⁴A_{2g}(F)→⁴T_{1g}(F) and ⁴A_{2g}(F)→⁴T_{2g}(F) of Cr³⁺, respectively, in an ordered octahedral environment in the LDH layer.^[23–25] The MCr–CO₃–LDH samples also show similar absorption maxima at 410 and 570 nm (Figure S3 in the Supporting Information). The small shift in the absorption band for these LDH materials might be due to the electronic competition among Cr^{III} and the M^{II} metal ions.^[23a] The broad absorption of these LDH materials motivated us to explore their potential photocatalytic activity with visible-light response.

As shown in Figure 2, the Cr-containing LDHs display broad absorption coverage in the region 350–800 nm; this indicates the feasibility of their utilization of visible light from sunlight. Sulforhodamine-B (SRB) and Congo Red were chosen as prototype molecules because of their high solubility in water and the resulting serious environmental problems.^[20,26] The absorption spectra of the solution as a function of irradiation time (at every 10 min interval over a period of 120 min for SRB) during the degradation process were recorded by using a UV/Vis spectrometer (Figure 3). During the whole photocatalytic process, the characteristic absorption band of SRB at approximately 565 nm decreased with no shift in peak wavelength. The self-degradation of SRB was also studied, and only approximately 3% SRB was photolyzed after 120 min irradiation without any catalyst. The existence of CO₃^{2–}-type LDH catalysts accelerate its photodegradation with the activity order of ZnCr–CO₃–LDH > CuCr–CO₃–LDH > NiCr–CO₃–LDH.

The calculated reaction constants were 2.30 × 10^{–5}, 6.50 × 10^{–6}, 3.30 × 10^{–6} min^{–1}, respectively. More interestingly, the NO₃[–]-type LDH catalysts exhibited much higher activity than the CO₃^{2–}-type LDH and P25, with the sequence CuCr–NO₃–LDH ≈ NiCr–NO₃–LDH > ZnCr–NO₃–LDH (reaction constants were 4.80 × 10^{–4}, 4.65 × 10^{–4}, 1.15 × 10^{–4} min^{–1}, respectively). SBR can be completely degraded

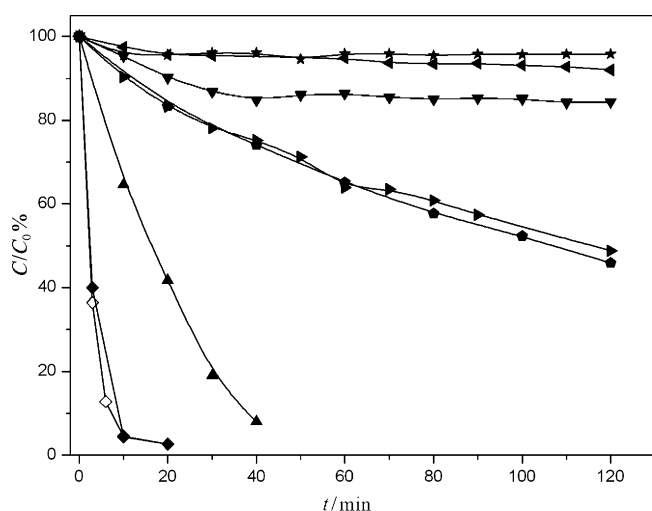


Figure 3. Photocatalytic degradation of SRB over MCr-X-LDHs (M = Cu, Ni, Zn) as a function of reaction time under visible light ($\lambda > 400$ nm). Samples: blank (*); NiCr-CO₃²⁻ (\blacktriangleleft); CuCr-CO₃²⁻ (\blacktriangledown); ZnCr-CO₃²⁻ (\blacktriangleright); P25 TiO₂, used as a reference (pentagon); ZnCr-NO₃⁻ (\blacktriangle); NiCr-NO₃⁻ (\blacklozenge); CuCr-NO₃⁻ (\diamond).

in 20 min with the use of CuCr-NO₃-LDH or NiCr-NO₃-LDH as the photocatalyst. Furthermore, the MCr-NO₃-LDHs were demonstrated to be excellent visible-light photocatalysts for the degradation of Congo Red. As shown in Figure S4 in the Supporting Information, MCr-NO₃-LDHs (M = Cu, Ni, Zn) showed removal capability of approximately 80% for Congo Red in 90 min, much greater than that of MCr-CO₃-LDHs and P25. In addition, colorless pollutants including phenols and chlorinated phenols have attracted much attention because of their widespread use in several industrial processes. 2,4,6-Trichlorophenol (2,4,6-TCP) and salicylic acid sodium were used to test the catalytic performance of LDHs. As shown in Figure 4, approxi-

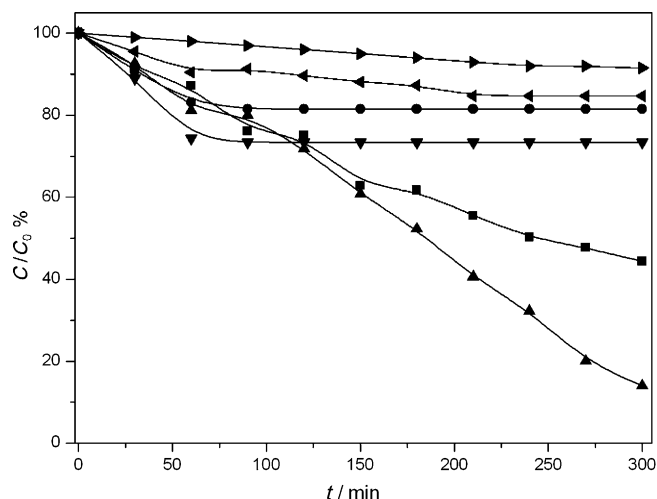


Figure 4. Photocatalytic degradation of 2,4,6-TCP over MCr-X-LDHs (M = Cu, Zn) as a function of reaction time under visible light ($\lambda > 400$ nm). TiO₂ was used as a reference sample. Samples: blank (\blacktriangleright); TiO₂, used as a reference (pentagon); CuCr-CO₃²⁻ (\bullet); ZnCr-CO₃²⁻ (\blacktriangledown); ZnCr-NO₃⁻ (\blacksquare); CuCr-NO₃⁻ (\blacktriangle).

mately 10% self-decomposition occurred for 2,4,6-TCP after 300 min irradiation without catalyst; in contrast, CuCr-NO₃-LDH and ZnCr-NO₃-LDH showed much higher photocatalytic activity than TiO₂ and CO₃²⁻-type LDH catalysts. The calculated reaction constants were $2.48 \times 10^{-5} \text{ min}^{-1}$ for CuCr-NO₃-LDH and $1.31 \times 10^{-5} \text{ min}^{-1}$ for ZnCr-NO₃-LDH. In the case of salicylic acid sodium, approximately 90% of contaminant was removed by CuCr-NO₃-LDH, which is superior to MCr-CO₃-LDHs and P25 (Figure S5 in the Supporting Information). Based on these results, it was found that the M^{II}Cr-NO₃-LDHs exhibit much higher photocatalytic activity than M^{II}Cr-CO₃-LDHs and even TiO₂ for the degradation of organic dyes as well as colorless pollutants.

It was well-known that the photocatalytic degradation of dye is a complicated process in which its adsorption on a catalyst surface is the first step.^[26] The excellent photocatalytic performance of MCr-NO₃-LDHs can be attributed to the surface electrical properties compared with MCr-CO₃-LDHs. As shown in Table 1, the MCr-NO₃-LDHs exhibited

Table 1. The ζ -potential [mV] of various Cr-containing LDHs dispersed in water (concentration: 0.06 mg mL⁻¹).

	CuCr	NiCr	ZnCr
NO ₃ ⁻	36.6	30.2	32.7
CO ₃ ²⁻	27.8	17.9	9.2

much higher ζ -potential (30.2–36.6 mV) than the MCr-CO₃-LDHs (9.2–27.8 mV). The superior surface potential of the MCr-NO₃-LDHs facilitates pollutant adsorption onto the LDH particles, which promotes the transfer of the light-generated charge carriers (OH groups) to the surface. Furthermore, the specific surface area of the Cr-containing LDHs was obtained by nitrogen sorption measurement (Table S1 in the Supporting Information). It was found that the values of these LDH materials are rather rule-less. No correlation between photocatalytic activity and specific surface area can be observed, which excludes the influence of specific surface area on the catalytic activity. Therefore, the surface electric property of these LDH materials plays a more important role in determining their photocatalytic activity.

The cyclic performance of these MCr-NO₃-LDH photocatalysts was also evaluated, and the catalysts can be easily separated and reused without any treatment. The photocatalytic activity of the MCr-NO₃-LDHs for the degradation of SRB maintained a high level even after 12 repeated measurements (220 min for CuCr-NO₃, 280 min for NiCr-NO₃, 500 min for ZnCr-NO₃-LDHs; Figure S6 in the Supporting Information). CuCr-NO₃-LDH also shows recyclable stability for the decomposition of 2,4,6-TCP and salicylic acid sodium (Figure S7 in the Supporting Information). Based on these results, it can be concluded that the MCr-NO₃-LDHs can serve as effective photocatalysts with high visible-light-response activity, long-term stability as well as excellent recycle ability.

Since the semiconductor property of layered hydroxide materials has rarely been reported, the excellent photocatalytic performance with visible-light-response attracted our research interest. In order to understand the redox ability of the LDHs, the spin-trapping electron spin resonance (ESR) technique was employed to investigate the presence of active radicals (the electron and hole) formed in the MCr-NO₃-LDHs. The surface OH group plays a key role in the photocatalytic reaction of dye molecule, owing to its acceptance of photohole to form hydroxyl radical ([•]OH), which is the principal reactive oxidant.^[5,6] Since OH groups are located on the surface of LDH materials,^[18] the catalysts can exhibit high photoactivity if the OH group is excited by light. Besides hydroxyl radicals, superoxide anion radicals (O₂^{•-}) also serve as primary oxidizing species in the photocatalytic oxidation process. The generation of active radicals ([•]OH and O₂^{•-}) from the MCr-NO₃-LDHs was confirmed by ESR with dimethylpyridine *N*-oxide (DMPO) as a spin-trapping reagent. As shown in Figure 5, the four characteristic

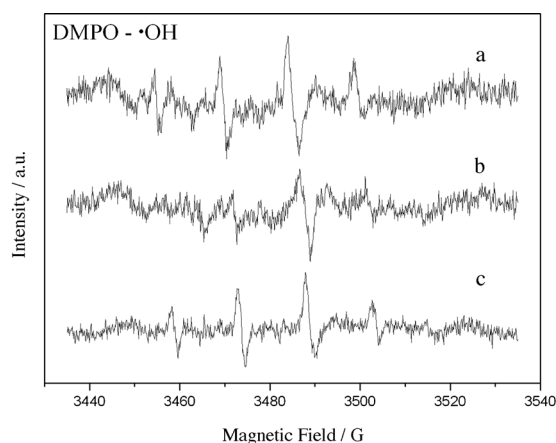


Figure 5. DMPO spin-trapping ESR spectra recorded for a) CuCr-NO₃-LDH, b) NiCr-NO₃-LDH, c) ZnCr-NO₃-LDH at ambient temperature in aqueous dispersion for DMPO-[•]OH ([DMPO]=0.10 M, *m*_{cat}=2 mg, *V*_{solvent}=0.5 mL, λ > 400 nm).

peaks for DMPO-[•]OH with intensity ratio of 1:2:2:1 were obviously observed when the samples were illuminated with visible light. As shown in Figure 6, the six characteristic peaks for DMPO-O₂^{•-} were observed in methanol. No signals were detected without irradiation; this indicates that [•]OH and O₂^{•-} radicals are formed through the activation of molecular oxygen in the photocatalytic process upon irradiation with visible light.^[16d] The photogenerated holes (*h*_{vb}⁺) as well as the transitions of electrons (*e*_{cb}⁻) occurred from the band gap in the Cr(OH)₆³⁺ during the photocatalytic process. The [•]OH originates from the reaction of *h*_{vb}⁺ with the OH group in the LDH layer; while the O₂^{•-} results from the reaction of *e*_{cb}⁻ with surface-absorbed O₂, as shown Equations (1)–(3).^[16]

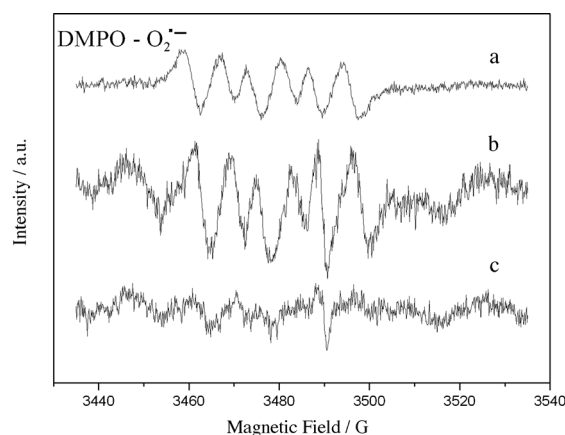
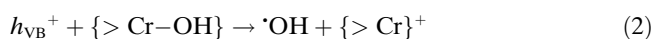


Figure 6. DMPO spin-trapping ESR spectra recorded for a) CuCr-NO₃-LDH, b) NiCr-NO₃-LDH, c) ZnCr-NO₃-LDH at ambient temperature in methanol dispersion for DMPO-O₂^{•-} ([DMPO]=0.10 M, *m*_{cat}=2 mg, *V*_{solvent}=0.5 mL, λ > 400 nm).



Compared with P25, the excellent photocatalytic activity of MCr-NO₃-LDH is possibly due to the large amount of OH groups on the LDH surface. Furthermore, it has been reported that O₂^{•-} participates in the regeneration of OH groups.^[27] The formation of O₂^{•-} on the LDH surface will generate the OH group and H₂O₂ [Eqs. (4)–(6)]. H₂O₂ can be further reduced by photoinduced electrons; this results in the promotion of [•]OH radical formation:^[16e–g]



As a result, the surface OH groups are recycled. Moreover, the high ζ-potential of MCr-NO₃-LDHs leads to strong adsorption of pollutants onto the surface of the catalyst, which can increase the efficiency of active [•]OH radicals and avoid the recombination of [•]OH and O₂^{•-}. The evidence that both DMPO-[•]OH and DMPO-O₂^{•-} are produced on MCr-LDHs provides a solid indication that the photogenerated charge carriers in the LDHs not only possess strong redox ability but are also long-lived enough to react with the surface adsorbed oxygen or H₂O.

It was found that the high dispersion of the CrO₆ octahedron in the LDH layer plays a key role in responding visible light and photogenerating charge carriers. Compared with the MCr-LDH samples, commercial Cr(OH)₃ also shows similar absorption maxima in the visible-light region (Figure S8 in the Supporting Information);^[17c,28] however, no photocatalytic performance with visible-light irradiation was observed, which is attributed to the aggregation state of octahedron CrO₆ in Cr(OH)₃. In contrast, the LDH matrix provides an ordered dispersion of the CrO₆ octahedron in

the layer; this promotes the efficiency of the excited electron and avoids the recombination of electron and hole.^[17a,18,23]

Scanning transmission electron microscopy (STEM) was employed to obtain further insight into the elemental distribution in the as-prepared MCr-LDHs. Figure 7a shows a

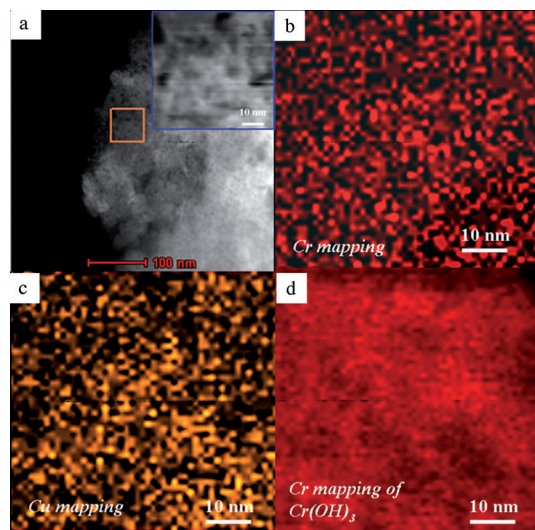


Figure 7. a) HADDF-STEM image of CuCr-NO₃-LDH. The inset shows the mapping area of the sample. Elemental mapping images of b) Cr, c) Cu for a sample of CuCr-NO₃-LDH, d) Cr mapping images for a sample of Cr(OH)₃.

high-angle annular dark field (HAADF) micrograph of CuCr-NO₃-LDH; Figure 7b and c display the elemental maps of Cr and Cu, respectively, from which a uniform and homogeneous distribution of both Cr and Cu was observed with a discrimination of 1–2 nm. In the case of Cr(OH)₃, however (Figure 7d), serious aggregation of Cr was found. Due to the instrumental limitation and detector noise during scanning, the atomic state of octahedron Cr was no longer discernable. The element maps disclose that the Cr and Cu are highly dispersive in the LDH matrix, which accounts for the visible-light-driven photocatalytic performances.

For the purpose of further understanding the electronic structure of the Cr-containing LDH materials and the resulting photocatalytic behavior, the band structure, the densities of states (DOS) as well as the partial densities of states (PDOS) for the ideal model of MCr-NO₃-LDHs were calculated by density functional theory (DFT) calculations. As shown in Figure 8a, it was found that the valence band (VB) maximum and conduction band (CB) minimum of CuCr-LDH are located at the same Z point=(0,0,1/2) of the Brillouin zone with a direct energy gap of about 1.6 eV; this indicates that the compound is a direct semiconductor. For direct semiconductors, generally, it is much easier to separate the electron-hole pair upon light excitation than the indirect case, which might lead to higher photocatalytic efficiency.^[29] Figure 8b shows the DOS and PDOS of CuCr-

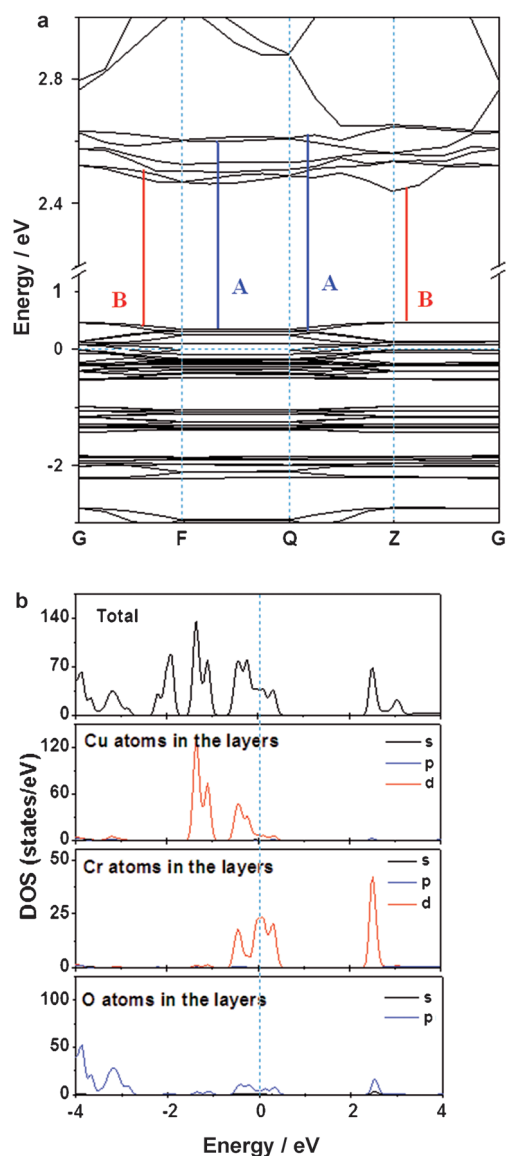


Figure 8. a) Band structure for CuCr-NO₃-LDH, and b) the total and partial density of states.

NO₃-LDH, from which it was found that the VB top is primarily constructed by the occupied Cr 3d orbitals (A_{2g}) while the CB bottom is mainly dominated by the unoccupied Cr 3d orbitals.

The band gap transitions from the top of the VB (highest occupied molecular orbital; HOMO) to the bottom of the CB (lowest unoccupied molecular orbital; LUMO) mainly occur from the occupied Cr 3d (A_{2g}) orbitals to unoccupied Cr 3d orbitals ($T_{2g}+T_{1g}$). Additionally, as illustrated in Figure 8a, the electronic structure of the CB bottom is composed of two parts (LUMO and LUMO+1) with slightly different band energies, which would result in different optical transitions.^[30] This is in accordance with the two strong visible-light absorption bands of the CuCr-NO₃-LDH (Figure 2). Transition A is responsible for the absorption band at 410 nm with higher transition energy (${}^4A_{2g}(F) \rightarrow$

$^4T_{1g}(F)$); while transition B corresponds to the absorption at 570 nm ($^4A_{2g}(F) \rightarrow ^4T_{2g}(F)$). It is noteworthy that the contribution of the O 2p orbitals in the LDH layers was also observed for both the HOMO and the LUMO, indicating a mixing of the O 2p and Cr 3d orbitals. This suggests that the CrO_6 octahedron in $CuCr-NO_3-LDH$ plays a key role in the photocatalytic activity. Based on our results, the $CuCr-NO_3-LDH$ material—crystallized in a $R3m$ rhombohedral symmetry with the specific CrO_6 arranged in the hydroxide layers—can serve as a visible-light-driven photocatalyst for the decomposition of pollutants, which facilitates the enhancement of light absorption efficiency.

In summary, a family of visible-light responsive $MCr-LDHs$ ($M=Cu, Ni, Zn$) was synthesized by a scale-up method (SNAS), which displays remarkable photocatalytic activity for RSB, Congo Red, chlorinated phenol and salicylic acid sodium under visible-light irradiation. The $MCr-NO_3-LDHs$ ($M=Cu, Ni$) exhibit 20-times higher photocatalytic activity than P25 as well as excellent recycle ability, owing to the high dispersion of the CrO_6 unit in the LDH matrix. The strong photocatalytic activity of Cr-containing LDHs is attributed to: 1) the low band gap, which causes the pronounced visible-light absorption; 2) the abundant surface OH groups, which accept photogenerated holes to yield highly reactive hydroxyl radicals. Energy band analysis indicates that $MCr-NO_3-LDHs$ show visible-light response originating from d–d transition in the orderly dispersed CrO_6 octahedron in the LDH layer. By virtue of the facile scale-up method and the intrinsic dispersion of the MO_6 octahedron unit, this approach can be extended for the preparation of other metal hydroxides or oxides with photocatalytic activity upon visible-light irradiation. Further studies with the LDH photocatalysts for the visible-light driven splitting of water into hydrogen are underway.

Acknowledgements

This project was supported by the 973 Program (grant no. 2011CBA00504), the National Natural Science Foundation of China, the 111 Project (grant no. B07004), and the Collaborative Project from the Beijing Education Committee.

Keywords: chromium • layered double hydroxides • MO_6 octahedron • photochemistry • visible-light response

- [1] N. Armaroli, V. Balzani, *Angew. Chem.* **2007**, *119*, 52; *Angew. Chem. Int. Ed.* **2007**, *46*, 52.
- [2] J. C. Crittenden, H. S. White, *J. Am. Chem. Soc.* **2010**, *132*, 4503.
- [3] a) A. Fujishima, K. Honda, *Nature* **1972**, *238*, 37; b) M. Grätzel, *Nature* **2001**, *414*, 338.
- [4] A. Hagfeldt, M. Grätzel, *Chem. Rev.* **1995**, *95*, 49.
- [5] a) G. Liu, Y. Zhao, C. Sun, F. Li, G. Q. Lu, H.-M. Cheng, *Angew. Chem.* **2008**, *120*, 4592; *Angew. Chem. Int. Ed.* **2008**, *47*, 4516; b) J. Tang, Z. Zou, J. Ye, *Angew. Chem.* **2004**, *116*, 4563; *Angew. Chem. Int. Ed.* **2004**, *43*, 4463; c) K. Maeda, N. Sakamoto, T. Ikeda, H. Ohtsuka, A. Xiong, D. Lu, M. Kanehara, T. Teranishi, K. Domen, *Chem. Eur. J.* **2010**, *16*, 7750.
- [6] a) T. L. Thompson, Jr., J. T. Yates, *Chem. Rev.* **2006**, *106*, 4428; b) M. R. Hoffmann, S. T. Martin, W. Choi, D. W. Bahnemann, *Chem. Rev.* **1995**, *95*, 69; c) M. Zhang, Q. Wang, C. Chen, L. Zang, W. Ma, J. Zhao, *Angew. Chem.* **2009**, *121*, 6197; *Angew. Chem. Int. Ed.* **2009**, *48*, 6081.
- [7] a) X. Chen, S. S. Mao, *Chem. Rev.* **2007**, *107*, 2891; b) C. Chen, W. Zhao, P. Lei, J. Zhao, N. Serpone, *Chem. Eur. J.* **2004**, *10*, 1956.
- [8] R. Asahi, T. Morikawa, T. Ohwaki, K. Aoki, Y. Taga, *Science* **2001**, *293*, 269.
- [9] S. U. M. Khan, M. Al-Shahry, W. B. Ingler, Jr., *Science* **2002**, *297*, 2243.
- [10] W. Zhao, W. Ma, C. Chen, J. Zhao, Z. Shuai, *J. Am. Chem. Soc.* **2004**, *126*, 4782.
- [11] X. Shu, Z. An, L. Wang, J. He, *Chem. Commun.* **2009**, *45*, 5901.
- [12] H. G. Yang, C. H. Sun, S. Z. Qiao, J. Zou, G. Liu, S. C. Smith, H. M. Cheng, G. Q. Lu, *Nature* **2008**, *453*, 638.
- [13] a) H. G. Yang, G. Liu, S. Z. Qiao, C. H. Sun, Y. G. Jin, S. C. Smith, J. Zou, H. M. Cheng, G. Q. Lu, *J. Am. Chem. Soc.* **2009**, *131*, 4078; b) X. Han, Q. Kuang, M. Jin, Z. Xie, L. Zheng, *J. Am. Chem. Soc.* **2009**, *131*, 3152; c) Y. Q. Dai, C. M. Cobley, J. Zeng, Y. M. Sun, Y. N. Xia, *Nano Lett.* **2009**, *9*, 2455; d) S. C. Chen, W. H. Ma, J. Zhao, *Chem. Soc. Rev.* **2010**, *39*, 4206; e) S. Sakthivel, H. Kisch, *Angew. Chem.* **2003**, *115*, 5057; *Angew. Chem. Int. Ed.* **2003**, *42*, 4908; f) H. G. Kim, P. H. Borse, W. Choi, J. S. Lee, *Angew. Chem.* **2005**, *117*, 4661; *Angew. Chem. Int. Ed.* **2005**, *44*, 4585.
- [14] a) C. G. Silva, Y. Bouzizi, V. Fornés, H. García, *J. Am. Chem. Soc.* **2009**, *131*, 13833; b) L. Teruel, Y. Bouzizi, P. Atienzar, V. Fornes, H. García, *Energy Environ. Sci.* **2010**, *3*, 154.
- [15] G. Liu, H. G. Yang, X. Wang, L. Cheng, J. Pan, G. Q. Lu, H.-M. Cheng, *J. Am. Chem. Soc.* **2009**, *131*, 12868.
- [16] a) X. Zong, H. Yan, G. Wu, G. Ma, F. Wen, L. Wang, C. Li, *J. Am. Chem. Soc.* **2008**, *130*, 7176; b) Z. Li, Z. Xie, Y. Zhang, L. Wu, X. Wang, X. Fu, *J. Phys. Chem. C* **2007**, *111*, 18348; c) Z. Li, T. Dong, Y. Zhang, L. Wu, J. Li, X. Wang, X. Fu, *J. Phys. Chem. C* **2007**, *111*, 4727; d) X. Fu, X. Wang, Z. Ding, D. Y. C. Leung, Z. Zhang, J. Long, W. Zhang, Z. Li, X. Fu, *Appl. Catal. B* **2009**, *91*, 67; e) A. A. Khodja, T. Sehili, J. Pilichowski, P. Bolue, *J. Photochem. Photobiol. A* **2001**, *141*, 231; f) H. Goto, Y. Hanada, T. Ohno, M. Matsumura, *J. Catal.* **2004**, *225*, 223; g) H. C. Yatmaz, A. Akyol, M. Bayramoglu, *Ind. Eng. Chem. Res.* **2004**, *43*, 6035.
- [17] a) J. J. Criado, B. Macias, V. Rives, *React. Kinet. Catal. Lett.* **1985**, *27*, 313; b) M. del Arco, M. J. Holgado, C. Martin, V. Rives, *Spectrosc. Lett.* **1987**, *20*, 201; c) L. Palmisano, V. Augugliaro, A. Sclafani, M. Schiavello, *J. Phys. Chem.* **1988**, *92*, 6710; d) C. Martin, I. Martin, V. Rives, L. Palmisano, M. Schiavello, *J. Catal.* **1992**, *134*, 434; e) A. Taguchi, F. Schüth, *Microporous Mesoporous Mater.* **2005**, *77*, 1; f) Z. Zhu, Z. Chang, L. Kevan, *J. Phys. Chem. B* **1999**, *103*, 2680; g) L. Spiccia, W. Marty, *Inorg. Chem.* **1986**, *25*, 266; h) J. Gómez-Morales, J. García-Carmona, R. Rodríguez-Clemente, D. Muraviev, *Langmuir* **2003**, *19*, 9110; i) B. M. Weckhuysen, I. E. Wachs, R. A. Schoonheydt, *Chem. Rev.* **1996**, *96*, 3327.
- [18] a) P. J. Sideris, U. G. Nilsen, Z. Gan, C. P. Grey, *Science* **2008**, *321*, 113; b) G. R. Williams, D. O'Hare, *J. Mater. Chem.* **2006**, *16*, 3065; c) D. G. Evans, X. Duan, *Chem. Commun.* **2006**, *42*, 485; d) E. A. Gardner, K. M. Huntoon, T. J. Pinnavaia, *Adv. Mater.* **2001**, *13*, 1263; e) J. B. Han, Y. B. Dou, M. Wei, D. G. Evans, X. Duan, *Angew. Chem.* **2010**, *122*, 2217; *Angew. Chem. Int. Ed.* **2010**, *49*, 2171; f) L. Li, R. Z. Ma, Y. Ebina, K. Fukuda, K. Takada, T. Sasaki, *J. Am. Chem. Soc.* **2007**, *129*, 8000; g) J. He, M. Wei, B. Li, Y. Kang, D. G. Evans, X. Duan, *Struct. Bonding (Berlin)* **2006**, *119*, 89.
- [19] a) L. Li, Y. Feng, Y. Li, W. Zhao, J. Shi, *Angew. Chem.* **2009**, *121*, 6002; *Angew. Chem. Int. Ed.* **2009**, *48*, 5888; b) Y. Zhi, Y. Li, Q. Zhang, H. Wang, *Langmuir* **2010**, *26*, 15546; c) E. M. Seftel, E. Popovici, M. Mertens, K. D. Witte, G. V. Tendeloo, P. Cool, E. F. Van-sant, *Microporous Mesoporous Mater.* **2008**, *113*, 296; d) D. P. De-becker, E. M. Gaigneaux, G. Busca, *Chem. Eur. J.* **2009**, *15*, 3920.
- [20] a) Y. Zhao, M. Wei, J. Lu, Z. L. Wang, X. Duan, *ACS Nano* **2009**, *12*, 4009; b) Y. Zhao, S. He, M. Wei, D. G. Evans, X. Duan, *Chem. Commun.* **2010**, *46*, 3031.

- [21] Y. Zhao, F. Li, R. Zhang, D. G. Evans, X. Duan, *Chem. Mater.* **2002**, *14*, 4286.
- [22] a) Y. Kobayashi, X. L. Ke, H. Hata, P. Schiffer, T. E. Mallouk, *Chem. Mater.* **2008**, *20*, 2374; b) J. Pisson, C. Taviot-Gueho, Y. Israeli, F. Leroux, P. Munsch, J. P. Itie, V. Briois, N. Morel-Desrosiers, J. P. Besse, *J. Phys. Chem. B* **2003**, *107*, 9243.
- [23] a) J. W. Bocclair, P. S. Braterman, *Chem. Mater.* **1998**, *10*, 2050; b) J. W. Bocclair, P. S. Braterman, J. Jiang, S. Lou, F. Yarberry, *Chem. Mater.* **1999**, *11*, 303; c) C. Taviot-Guého, F. Leroux, C. Payen, J. P. Besse, *Appl. Clay Sci.* **2005**, *28*, 111; d) H. Roussel, V. Briois, E. Elkaim, A. de Roy, J. P. Besse, *J. Phys. Chem. B* **2000**, *104*, 5915.
- [24] J. M. García-García, M. E. Perez-Bernal, R. J. Ruano-Casero, V. Rives, *Solid State Sci.* **2007**, *9*, 1115.
- [25] H. Roussel, V. Briois, E. Elkaim, A. D. Roy, J. P. Besse, *J. Phys. Chem. B* **2000**, *104*, 5915.
- [26] a) G. Liu, X. Li, J. Zhao, *Environ. Sci. Technol.* **2000**, *34*, 3982; b) T. Wu, G. Liu, J. Zhao, H. Hidaka, N. Serpone, *J. Phys. Chem. B* **1999**, *103*, 4862.
- [27] J. Araña, V. M. Rodriguez Lopez, J. M. Dona Rodriguez, J. A. Herrera Melian, J. Perez Pena, *Catal. Today* **2007**, *129*, 185.
- [28] P. McCarthy, J. Lauffenburger, P. Skonezny, D. Rohrer, *Inorg. Chem.* **1981**, *20*, 1566.
- [29] J. Huang, K. Ding, Y. Hou, X. Wang, X. Fu, *ChemSusChem* **2008**, *1*, 1011.
- [30] A. H. Reshak, S. Auluck, I. V. Kityk, X. Chen, *J. Phys. Chem. B* **2009**, *113*, 9161.

Received: June 20, 2011
Published online: October 11, 2011